

JOURNAL OF GLACIOLOGY



CAMBRIDGE
UNIVERSITY PRESS

THIS MANUSCRIPT HAS BEEN SUBMITTED TO THE JOURNAL OF GLACIOLOGY AND HAS NOT BEEN PEER-REVIEWED.

Extended ISMIP6 projections for the Antarctic ice sheet with the model SICOPOLIS

Journal:	<i>Journal of Glaciology</i>
Manuscript ID	JOG-21-0083
Manuscript Type:	Article
Date Submitted by the Author:	20-Jun-2021
Complete List of Authors:	Chambers, Christopher; Hokkaido University Institute of Low Temperature Science, Glaciology Greve, Ralf; Hokkaido University, Institute of Low Temperature Science; Hokkaido University Arctic Research Center Obase, Takashi; The University of Tokyo Atmosphere and Ocean Research Institute Saito, Fuyuki; Japan Agency for Marine-Earth Science and Technology Yokohama Institute for Earth Sciences, RIGC Abe-Ouchi, Ayako; The University of Tokyo Atmosphere and Ocean Research Institute
Keywords:	Ice-sheet modelling, Antarctic glaciology, Ice and climate
Abstract:	Ice-sheet simulations of Antarctica extending to the year 3000 are analysed to investigate the long-term impacts of 21st century warming. Climate projections are used as forcing until 2100 and afterwards no climate trend is applied. Fourteen experiments are for the "unabated warming" pathway, and three are for the "reduced emissions" pathway.

	<p>For the unabated warming path simulations, West Antarctica suffers a much more severe ice loss than East Antarctica. In these cases, the mass loss amounts to a 14 experiment average of ~ 3.5 m sea-level equivalent by the year 3000 and ~ 5.3 m for the most sensitive experiment. Four phases of mass loss occur during the collapse of the West Antarctic Ice Sheet. For the reduced emissions pathway, the mean mass loss is ~ 0.24 m sea-level equivalent. By demonstrating that the consequences of the 21st century unabated warming path forcing are large and long-term, the results present a different perspective to ISMIP6 (Ice Sheet Model Intercomparison Project for CMIP6). Extended ABUMIP (Antarctic BUttrressing Model Intercomparison Project) simulations, assuming sudden and sustained ice-shelf collapse, with and without bedrock rebound corroborate a negative feedback for ice loss found in previous studies.</p>

SCHOLARONE™
Manuscripts

Extended ISMIP6 projections for the Antarctic ice sheet with the model SICOPOLIS

Christopher CHAMBERS,^{1*} Ralf GREVE,^{1,2} Takashi OBASE,³ Fuyuki SAITO,⁴

Ayako ABE-OUCHI³

¹*Institute of Low Temperature Science, Hokkaido University, Sapporo, Japan*

²*Arctic Research Center, Hokkaido University, Sapporo, Japan*

³*Atmosphere and Ocean Research Institute, The University of Tokyo, Kashiwa, Japan*

⁴*Japan Agency for Marine-Earth Science and Technology, Yokohama, Japan*

Correspondence: Christopher Chambers <youstormorg@gmail.com>

ABSTRACT. Ice-sheet simulations of Antarctica extending to the year 3000 are analysed to investigate the long-term impacts of 21st century warming. Climate projections are used as forcing until 2100 and afterwards no climate trend is applied. Fourteen experiments are for the “unabated warming” pathway, and three are for the “reduced emissions” pathway. For the unabated warming path simulations, West Antarctica suffers a much more severe ice loss than East Antarctica. In these cases, the mass loss amounts to a 14 experiment average of ~ 3.5 m sea-level equivalent by the year 3000 and ~ 5.3 m for the most sensitive experiment. Four phases of mass loss occur during the collapse of the West Antarctic Ice Sheet. For the reduced emissions pathway, the mean mass loss is ~ 0.24 m sea-level equivalent. By demonstrating that the consequences of the 21st century unabated warming path forcing are large and long-term, the results present a different perspective to ISMIP6 (Ice Sheet Model Intercomparison Project for CMIP6), which saw only modest losses, or even slight gains, by the year 2100. Extended ABUMIP (Antarctic BUtressing Model Intercomparison Project) simulations, assuming sudden and sustained ice-shelf collapse, with and without bedrock rebound corroborate a

*Present address: Institute of Low Temperature Science, Hokkaido University, Sapporo, Japan.

27 **negative feedback for ice loss found in previous studies.**

28 1 INTRODUCTION

29 The Antarctic ice sheet (AIS) contains more than half of the Earth's freshwater, enough to raise sea levels
30 by 58 metres (Fretwell and others, 2013). An ice mass of 7.4 mm sea-level equivalent (SLE) was lost from
31 the AIS between 1992 and 2017 (The IMBIE team, 2018), and there is evidence to suggest that parts of
32 the West Antarctic Ice Sheet (WAIS) may already have begun an irreversible retreat (Joughin and others,
33 2014; Rignot and others, 2014).

34 The possibility of WAIS retreat and collapse was first presented by Mercer (1968) and there is pa-
35 leoclimatic evidence that it collapsed during past warm periods (Pollard and DeConto, 2009; Alley and
36 others, 2015; Dutton and others, 2015; Gasson and others, 2016; Turney and others, 2020). In contrast to
37 the East Antarctic Ice Sheet (EAIS), the WAIS is grounded on a bed that is mostly well below sea level
38 (Fig. 1) making it primarily a marine ice sheet. The WAIS bedrock bathymetry also deepens inward in
39 many areas, making it susceptible to marine-ice-sheet instability (e.g. Schoof, 2007). The WAIS is bounded
40 by the two largest ice shelf systems in the world, the Ross and the Ronne-Filchner which currently act to
41 buttress the grounded ice sheet (e.g. Joughin and Alley, 2011) and reduce ice flow across enormously long
42 below-sea-level grounding lines.

43 To estimate the future sea-level-rise contribution from the Antarctic and Greenland ice sheets until the
44 end of the 21st century, the Coupled Model Intercomparison Project Phase 6 (CMIP6) (Eyring and others,
45 2016) includes the Ice Sheet Model Intercomparison Project for CMIP6 (ISMIP6; Nowicki and others,
46 2016, 2020). ISMIP6 uses future climate scenarios as forcing for ice-sheet models including the SIMulation
47 COde for POLythermal Ice Sheets (SICOPOLIS; Greve and SICOPOLIS Developer Team, 2021) used here.
48 The set-up and results of the Antarctica ISMIP6 projections are described in Seroussi and others (2020),
49 and the results specifically obtained with SICOPOLIS are in Greve and others (2020). ISMIP6 found an
50 Antarctic mass loss of between -7.8 and 30.0 cm SLE from 2015 to 2100 under the “unabated warming
51 path” of Representative Concentration Pathway (RCP) 8.5 (Seroussi and others, 2020). The WAIS had an
52 overall mass loss of up to 18.0 cm SLE, while the EAIS mass change varied between -6.1 and 8.3 cm. The
53 results for the RCP2.6 pathway (that represents substantial emissions reductions) lie within the uncertainty
54 interval of the results for RCP8.5. Payne and others (2021) compared the impact of CMIP5 and CMIP6

55 forcings and found that the projected sea-level contribution at 2100 under the CMIP6 scenarios falls within
56 the CMIP5 range for the AIS. Edwards and others (2021) explored the uncertainty of the projections in
57 greater detail by using statistical emulation of the ice-sheet models, which allowed considering a much
58 larger range of climate scenarios and forcings. This study essentially confirmed the ISMIP6 findings: By
59 2100, the AIS does not show a clear response due to the competing processes of increasing ice loss and
60 snowfall accumulation, with possibilities encompassing the range from a significant mass loss to a slight
61 mass gain.

62 While the ISMIP6 projections extend to the year 2100, other studies have investigated longer term
63 AIS change. To do this some have used statistical relationships between past temperatures and global sea
64 levels (Levermann and others, 2013; Schaeffer and others, 2012). Alternatively Golledge and others (2015)
65 demonstrated using simulations that atmospheric warming in excess of 1.5 to 2 °C above present, triggers
66 ice-shelf collapse and a centennial to millennial-scale response in the AIS. They simulated a contribution to
67 sea-level-rise from Antarctica under higher emission scenarios of 0.6 to 3 metres by the year 2300. Similarly
68 Garbe and others (2020) found that at greater than 2 °C of global average warming, the WAIS is committed
69 to long-term partial collapse. They also found distinct regimes in the rates of sea-level rise per degree, with
70 a doubling in the rate if warming becomes greater than 2 °C. Lipscomb and others (2021) used ISMIP6
71 forced sensitivity simulations extended to year 2500 under a constant climate to evaluate the Antarctic
72 response to ocean forcing. They found long-term retreat of the WAIS and showed that the Amundsen sector
73 exhibits threshold behaviour with modest retreat or complete collapse depending on parameter settings.
74 The Antarctic BUttrressing Model Intercomparison Project (ABUMIP; Sun and others, 2020) compared
75 ice-sheet model responses to a removal of ice-shelf buttressing by investigating the scenario of sudden and
76 sustained loss of ice shelves and found that all models effectively lost a large part of WAIS over the 500
77 year long simulations. These studies point to threshold behaviour in the WAIS in response to atmosphere
78 and ocean warming.

79 Given the limited response of the AIS in the 21st century found in ISMIP6, the goal of our study is
80 to investigate the extended effects of the climate projections used in ISMIP6. To do this we simulate the
81 evolution of the AIS until the year 3000. Until 2100, we follow the ISMIP6 protocol, whereas afterwards
82 we assume a steady, late-21st-century climate without any further trend. In this longer-term perspective, a
83 very different picture emerges compared to the 21st century ISMIP6 findings. The remainder of this paper
84 is divided into four sections. Firstly the method is outlined in Section 2, followed by an analysis of the

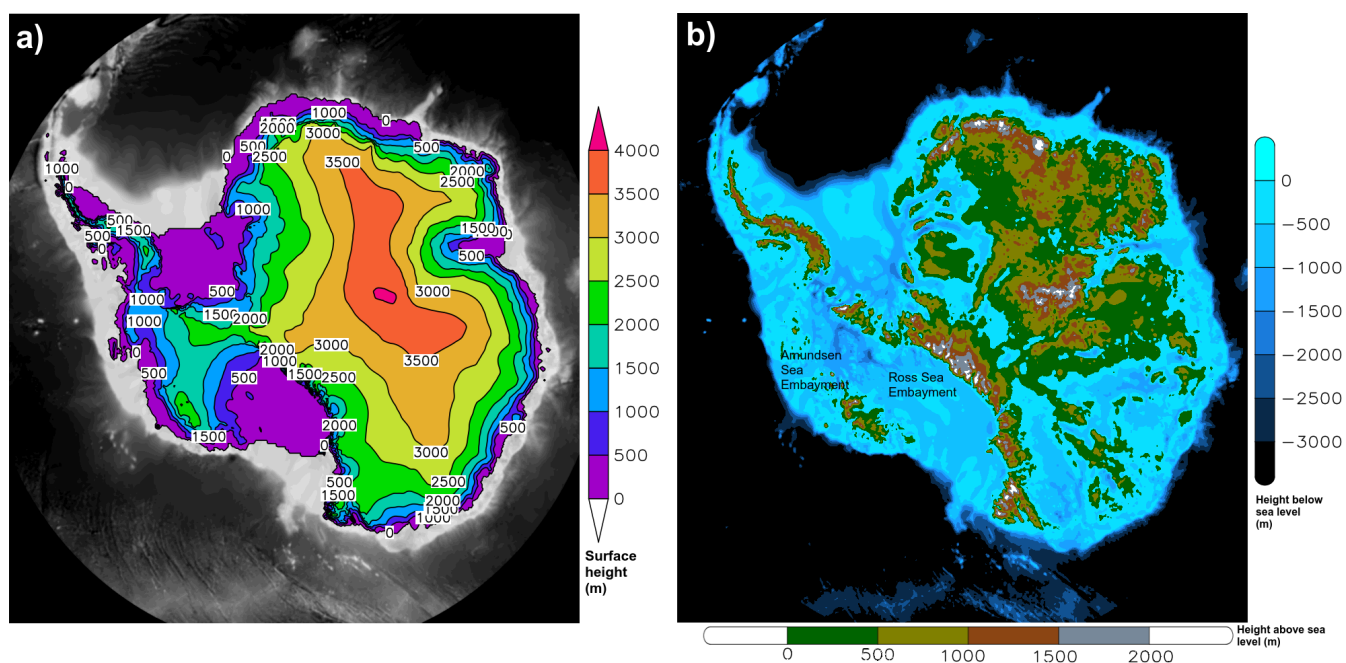


Fig. 1. SICOPOLIS year 2015 a) simulated surface topography and b) bedrock elevation above and below sea level. The bedrock elevation is from Bedmap2 (Fretwell and others, 2013) mapped onto the 8 km grid.

85 simulations in Section 3. Thirdly, the results are evaluated in Section 4, and finally a summary is provided
 86 in Section 5.

87 2 METHODS

88 SICOPOLIS, a polythermal ice-sheet model originally created by Greve (1995, 1997), is used to extend the
 89 ISMIP6 experiments to the year 3000. Here, we use version 5-dev, revision develop_63_rv5.1-62-g3c25a05
 90 (Greve and SICOPOLIS Developer Team, 2021). The simulation set-up for ISMIP6 is described in Greve
 91 and others (2020) and only summarized here. The model domain covers the entirety of Antarctica on
 92 an 8 km horizontal resolution regular (structured) grid based on a polar stereographic projection, with
 93 81 terrain-following ice layers and 41 lithosphere layers. The shallow-ice approximation is used for slow-
 94 flowing grounded ice. Hybrid shallow-ice-shelfy-stream dynamics, in the modified form of Bernales and
 95 others (2017), is used for fast-flowing grounded ice and the shallow-shelf approximation (SSA) is used for
 96 floating ice. The basal sliding coefficient is chosen differently for the 18 IMBIE (Ice sheet Mass Balance
 97 Inter-comparison Exercise) 2016 basins (Rignot and Mouginot, 2016) to optimize the agreement between
 98 simulated and observed present-day surface velocities (Greve and others, 2020, Sect. 3.2.3).

99 To obtain the reasonable initial state of the ice sheet shown in Figure 1a, a paleoclimatic spin-up

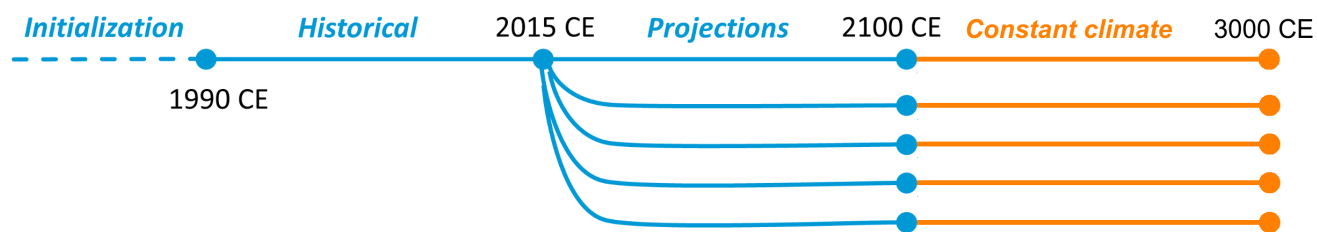


Fig. 2. Experimental design. Initialization is followed by a historical simulation from 1990 until 2015. ISMIP6 projections run from 2015 until the end of 2100. From 2100 to 3000 no further trend is applied. (Credit: edit of Figure 1 in Greve and others (2020), originally by Martin Rückamp, AWI Bremerhaven, Germany.)

100 simulation is run over a full glacial cycle (140 ka) to the year 1990 as described in Greve and others (2020,
 101 Sect. 3.2). There are then 25 years remaining to get to year 2015, which marks the start date of the
 102 ISMIP6 projections, so an additional simulation referred to as “Historical” in Figure 2, is run that applies
 103 NorESM1-M RCP8.5 surface mass balance, surface temperature anomalies, and oceanic forcing, to the
 104 1960–1989 climatology Greve and others (2020, Sect. 4.1).

105 The ISMIP6 projections run from 2015 to 2100 with atmospheric forcing consisting of anomalies of
 106 surface mass balance and temperature from a 1995 to 2014 climatology (Barthel and others, 2020; Nowicki
 107 and others, 2020; Seroussi and others, 2020; Payne and others, 2021). After 2100, the atmospheric forcing
 108 for the 10-year interval 2091–2100 is randomly sampled such that no further warming trend is applied
 109 (similar to Calov and others, 2018) but some year to year fluctuations remain. With the surface mass
 110 balance and temperature fixed on this 10-year period, they remain unchanged even if the topography of
 111 ice changes over the remaining 900 years. Ice-shelf basal melt rates are calculated using the non-local
 112 quadratic melt-rate parameterization of the “ISMIP6 standard approach”, driven by extrapolating the
 113 oceanic thermal forcing into the ice-shelf cavities (Jourdain and others, 2020). Beyond 2100, it is kept
 114 fixed at 2100 values.

115 All simulations are listed in Table 1. Fourteen experiments are for the 21st century “unabated warming
 116 path” RCP8.5 (CMIP5) / SSP5-8.5 (Shared Socioeconomic Pathways, CMIP6), and three are for the
 117 RCP2.6/SSP1-2.6 pathway that represents substantial emissions reductions and a maintenance of the
 118 global mean temperature below a 2 °C increase. In addition a control simulation (‘ctrl_proj’) uses constant
 119 climate conditions based on a 1995–2014 climatology and the present day oceanic forcing.

120 Using the NorESM1-M RCP8.5 forcing, “High” and “Low” melt-rate calibrations are tested, as well
 121 as a calibration (“PIGL-medium”) that applies observed basal-melt rates near the grounding line of the

Table 1. ISMIP6 future climate experiments discussed in this study. See Nowicki and others (2020) for references for the GCMs and Greve and others (2020) for further detail on the SICOPOLIS application of the experiments.

CMIP5 simulations		
Scenario	GCM	Ocean forcing
RCP8.5	NorESM1-M	Medium
RCP8.5	MIROC-ESM-CHEM	Medium
RCP2.6	NorESM1-M	Medium
RCP8.5	CCSM4	Medium
RCP8.5	NorESM1-M	High
RCP8.5	NorESM1-M	Low
RCP8.5	CCSM4 (ice-shelf collapse)	Medium
RCP8.5	NorESM1-M	PIGL-Medium
RCP8.5	HadGEM2-ES	Medium
RCP8.5	CSIRO-Mk3.6.0	Medium
RCP8.5	IPSL-CM5A-MR	Medium
RCP2.6	IPSL-CM5A-MR	Medium
CMIP6 simulations		
SSP5-8.5	CNRM-CM6-1	Medium
SSP1-2.6	CNRM-CM6-1	Medium
SSP5-8.5	UKESM1-0-LL	Medium
SSP5-8.5	CESM2	Medium
SSP5-8.5	CNRM-ESM2-1	Medium
Control simulation		
None (ctrl_proj)	1960-1989 climatology	Medium

122 Pine Island ice shelf under all ice shelves (Jourdain and others, 2020). One experiment, “CCSM4/RCP8.5
123 ice-shelf collapse”, accounts for ice-shelf fracture triggered by surface melting by implementing a time-
124 dependent ice-shelf-collapse mask. It assumes that collapse occurs following a 10-year period with annual
125 surface melt above 725 mm (Trusel and others, 2015).

126 In addition to the extended ISMIP6 simulations, the Antarctic BUttrressing Model Intercomparison
127 Project (ABUMIP; Sun and others, 2020) simulations are also extended to the year 3000. ABUMIP
128 compares ice-sheet model responses to a removal of ice-shelf buttressing by investigating the scenario of
129 sudden and sustained loss of ice shelves. This was designed to show the full potential of marine-ice-
130 sheet instability. The experiments are initialized from the simulated 1990 state of Antarctica. The original
131 ABUMIP simulations were run for 500 years and here we extend them a further 500 years. The simulations
132 are run with and without bedrock rebound (glacial isostatic adjustment). There are five experimental set-
133 ups as summarized below (for further detail see Sun and others, 2020):

134 (1) Control run (abuc): 1990 (initial) forcing is applied for the duration of the simulation.

135 (2) Ice-shelf removal or ‘float-kill’ (abuk) with no bedrock rebound: All floating ice is removed at the
136 simulation start and then continuously throughout the simulation. The bed topography remains fixed
137 at 1990 levels.

138 (3) Ice-shelf removal or ‘float-kill’ with bedrock rebound (abukiso): The same experiment as in (2) but
139 including glacial isostatic adjustment (GIA) using an elastic-lithosphere-relaxing-asthenosphere (ELRA)
140 model (parameters by Sato and Greve, 2012).

141 (4) Extreme sub-shelf melt and no bedrock rebound (abum): Applies an extremely high melt rate of
142 400 m a^{-1} underneath floating ice for a period of 500 years. This experiment acts as an alternative
143 to the more extreme abuk and also inevitably leads to a rapid loss of all ice shelves.

144 (5) Extreme sub-shelf melt with bedrock rebound (abumiso): As experiment (4) but including GIA as in
145 (3).

146 3 RESULTS

147 3.1 Extended ISMIP6 experiments

148 For the ISMIP6 extended experiments, the SLE contribution due to ice-mass melt is shown in Figure 3.
149 The graph is divided into 4 phases to roughly designate periods where the rates of SLE change tend to
150 be relatively constant. Over the ISMIP6 original experiment range, which ends at 2100 (within phase 1),
151 there is just a small, and uncertain, contribution to SLE. Throughout the 21st century the experiments
152 are identical to those for ISMIP6 so this small section of the graph is equivalent to Greve and others
153 (2020, Fig. 8). Beyond 2100, under a no-longer warming climate, the high-emission scenarios transition to
154 a period of relatively constant SLE change (phase 2). The onset of phase 2 varies between the cases from
155 the latter half of the 21st century to the early 22nd century. A third phase then begins as the rate of SLE
156 contribution increases. This phase is the period of most rapid ice-sheet mass-loss and there is a fair degree
157 of variability between the simulations in both the timing of the transition from phase 2 to 3 (between years
158 2340 and 2560), and in the level of SLE contribution at which this phase begins. A fourth and final phase
159 then begins as the SLE contribution levels out, which on average produces an end SLE contribution for
160 the high-emissions cases of ~ 3.5 m by the year 3000. Most of the cases are clustered close to this value
161 with all but two within ± 0.4 m. This is similar to a ~ 3.3 m value found in Bamber and others (2009) who
162 calculated the potential SLE contribution due to WAIS collapse by identifying grid cells below sea level on
163 retrograde bed slopes to infer the limit of grounding line retreat.

164 To investigate the causes of these apparent ice-sheet mass-loss regime shifts between the four phases,
165 here we analyse a representative case in more detail. The MIROC-ESM-CHEM RCP8.5 case lies within the
166 cluster of cases close to the mean of the unabated 21st century warming (RCP8.5/SSP5-8.5) runs (Fig. 3).
167 For this case the phase onsets occur for phase 2 around ~ 2100 , phase 3 around ~ 2350 and phase 4 at
168 ~ 2500 .

169 Figure 4 shows that simulated ice-mass loss is dominated by WAIS change and it is here where the
170 causes of the phase changes can be found. The transition from phase 1 to phase 2 is associated with the
171 period when the Ross Ice Shelf has retreated to such a point that the Ross Sea Embayment begins a more
172 rapid ice loss due to a reduction in the buttressing from the ice shelf (Fig. 4b). The transition to phase
173 3 occurs as, in addition to continued Ross Sea Embayment mass loss, the Amundsen Sea Embayment
174 begins a rapid retreat along its inward sloping grounding lines (Fig. 4c). Phase 4 is then associated with a

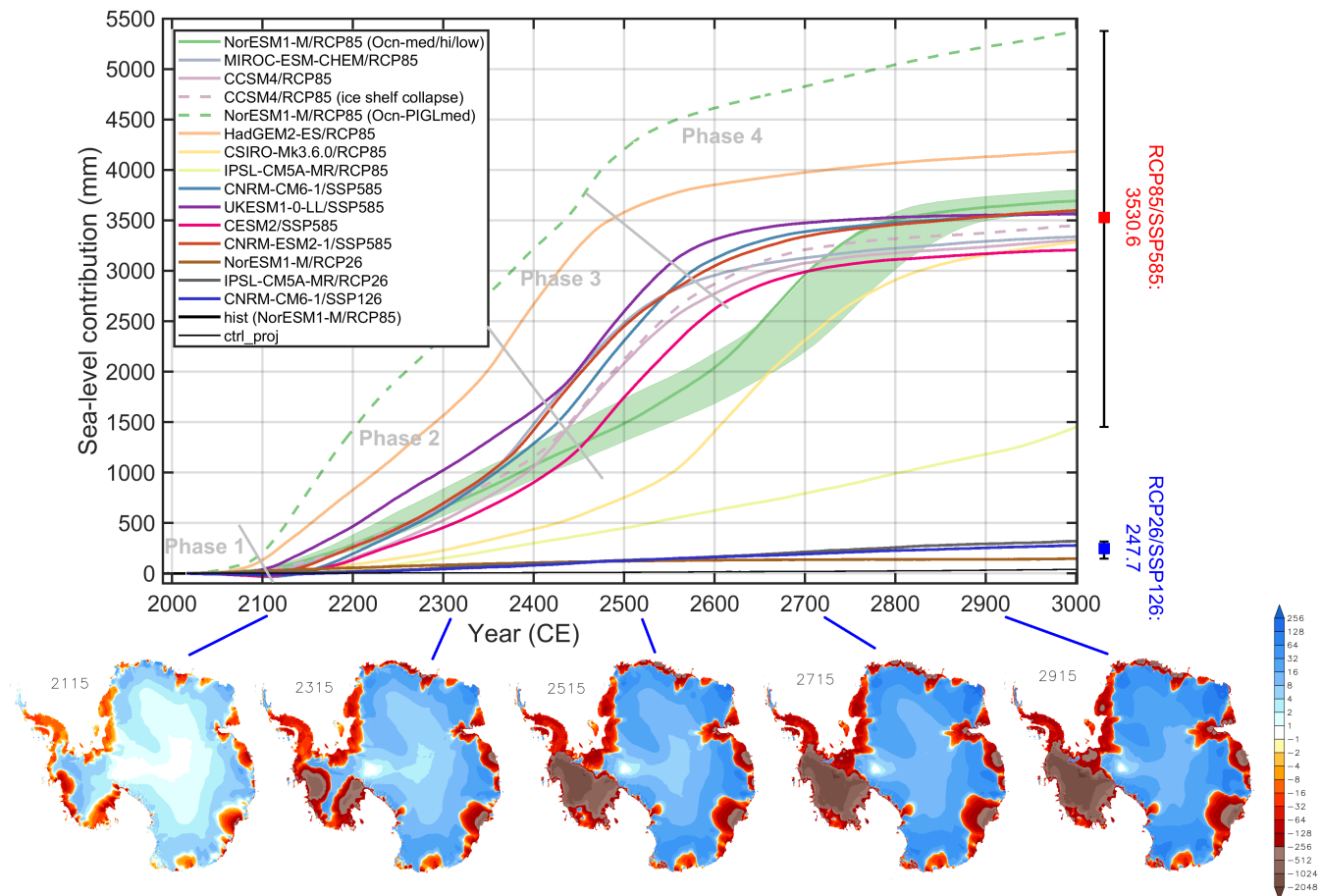


Fig. 3. Simulated ice mass change, counted positively for loss and expressed as sea-level equivalent (SLE) contribution. Phases mentioned in the text are labeled and grey lines are rough guides to denote the phase transitions. The red and blue boxes to the right show the means for RCP8.5/SSP5-8.5 and RCP2.6/SSP1-2.6, respectively; the whiskers show the full ranges. Below are ice surface elevation differences from 2015 (m) for the year indicated for case MIROC-ESM-CHEM RCP8.5.

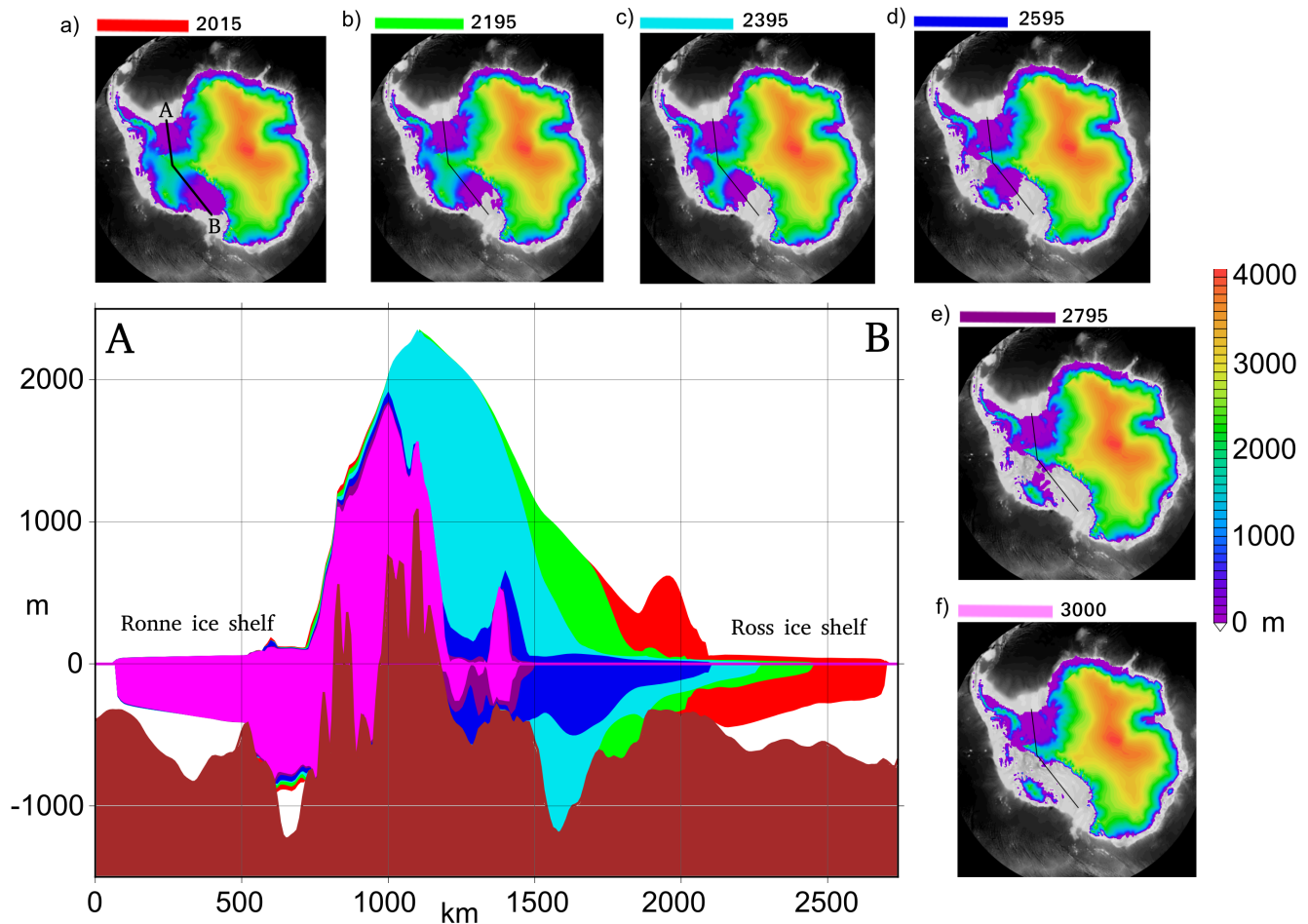


Fig. 4. West Antarctica vertical cross-section for simulation MIROC-ESM-CHEM RCP8.5 showing the colour-coded ice extent for the years labeled in the side plots (a to f) that show the ice surface elevation for the year indicated.

175 levelling-off in the SLE contribution as the WAIS is reduced to such an extent that the loss of the remaining
 176 ice grounded below sea level begins to contribute less and less to the SLE contribution (Fig. 4d-f).

177 In Figure 4 cross-sections through the ice along two connected diagonals through the WAIS are shown
 178 for the 6 times in the side panels a-f. This cross-section presents a roughly flow-line oriented view from the
 179 Ronne-Filchner Ice Shelf on the left, where minimal melt occurs, to the Ross Ice Shelf on the right where
 180 collapse occurs.

181 The greatest change to the topography in the cross-section occurs between the 2395 and 2595 cross-
 182 sections during which time a large ice shelf develops above a retrograde slope in the bed topography. The
 183 outer edge of this ice shelf lies inward of the original Ross Ice Shelf area which is now devoid of ice. It is
 184 also during this period when the peak elevation of the cross-section drops by about 400 m with very little

185 change either before or after.

186 An alternative cross-section across the WAIS that includes part of the EAIS is shown in Figure 5 (cross-
187 section location on inset in panel b) for four years that are chosen to highlight the key phases of retreat. At
188 the initialization time (2015, Fig. 5a) the WAIS is grounded on bedrock with just a sliver of liquid water
189 in the middle where the cross-section crosses the deep interior of the Ross Ice Shelf. During phase 1 the
190 ice-sheet profile changes little, then during phase 2, ocean melting undercuts the WAIS from the Ross Ice
191 Shelf into the Ross Sea Embayment. The surface elevation drops rapidly where this undercutting occurs,
192 as shown for 2395 in Figure 5b. As the Amundsen Sea Embayment also loses ice, the central WAIS ridge
193 becomes narrower.

194 During phase 3 the central ridge then collapses as ice mass is evacuated due to the compounding losses
195 from the Amundsen and Ross Sea Embayments. Phase 3 transitions to phase 4 not when all the WAIS ice
196 has melted but rather when the ice mass has been reduced to such an amount that further melt contributes
197 little to sea level as indicated in Figure 5c. Beyond that the remainder of WAIS ice, now mostly detached
198 from the bedrock can melt while contributing little to sea level in phase 4. The EAIS exhibits very little
199 change in the cross-section and the slight thickening is evident on very close inspection.

200 A cross-section through the Amundsen Embayment from the Pine Island Glacier and Thwaites Glacier
201 area up to the WAIS ridge is shown in Figure 6. The greatest loss of ice is seen between the 2195 and 2595
202 sections however the greatest ice edge retreat is between 2395 and 2795 because of the formation of ice
203 shelves, the most prominent of which is seen in the 2395 cross-section. The initial ice shelf, the 2395 ice
204 shelf, and another at 2595 all appear to be related to shallow areas in the bedrock that act to pin the shelf
205 and restrain the ice behind. The precarious nature of the present day ice extent is evident in the drop in
206 bedrock from the ice edge to about 490 km along the section.

207 The bedrock in the cross-section is plotted for 2015. By the latter stages in the simulation the bedrock
208 has lifted slightly, and the apparent narrow undercut in the ice seen in 2795 and 3000 between 800 and
209 900 km along the cross-section, is a consequence of this uplift rather than representing sea water undercut-
210 ting the ice.

211 A comparison between the three low-emission simulations with their high-emission counterparts is made
212 in Figure 7. For all of the low-emission cases there is very little noticeable change in the topography of the
213 ice sheet as a whole, consistent with the only small contribution to sea-level from these cases (Fig. 3). For
214 the high-emission cases, all show large losses in the WAIS with the greatest losses seen in the only CMIP6

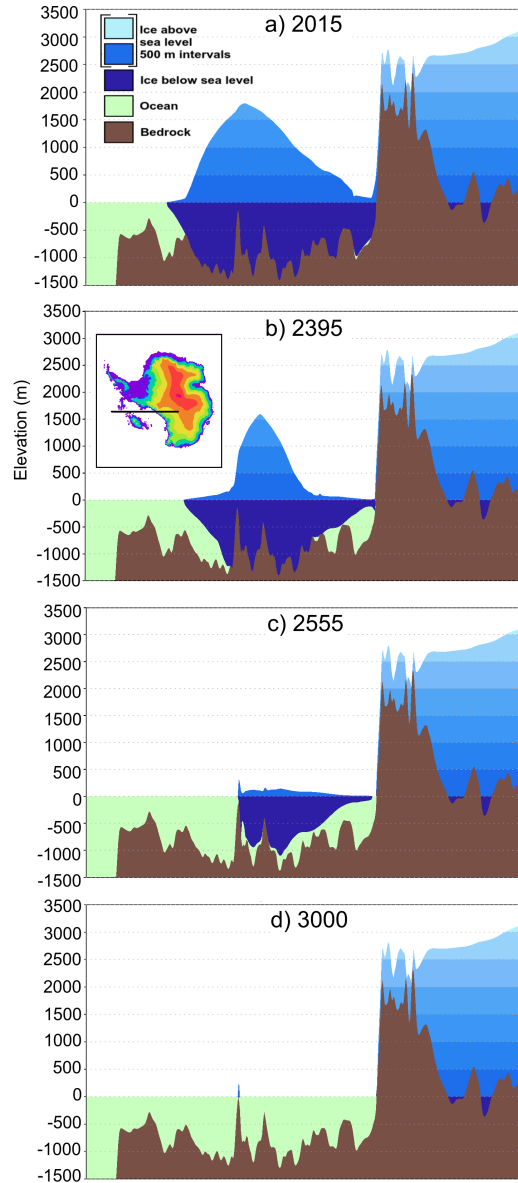


Fig. 5. Ice cross-sections for simulation MIROC-ESM-CHEM RCP8.5 for a) 2015, b) 2395, c) 2555, and d) 3000 across the black line shown on inset panel of b).

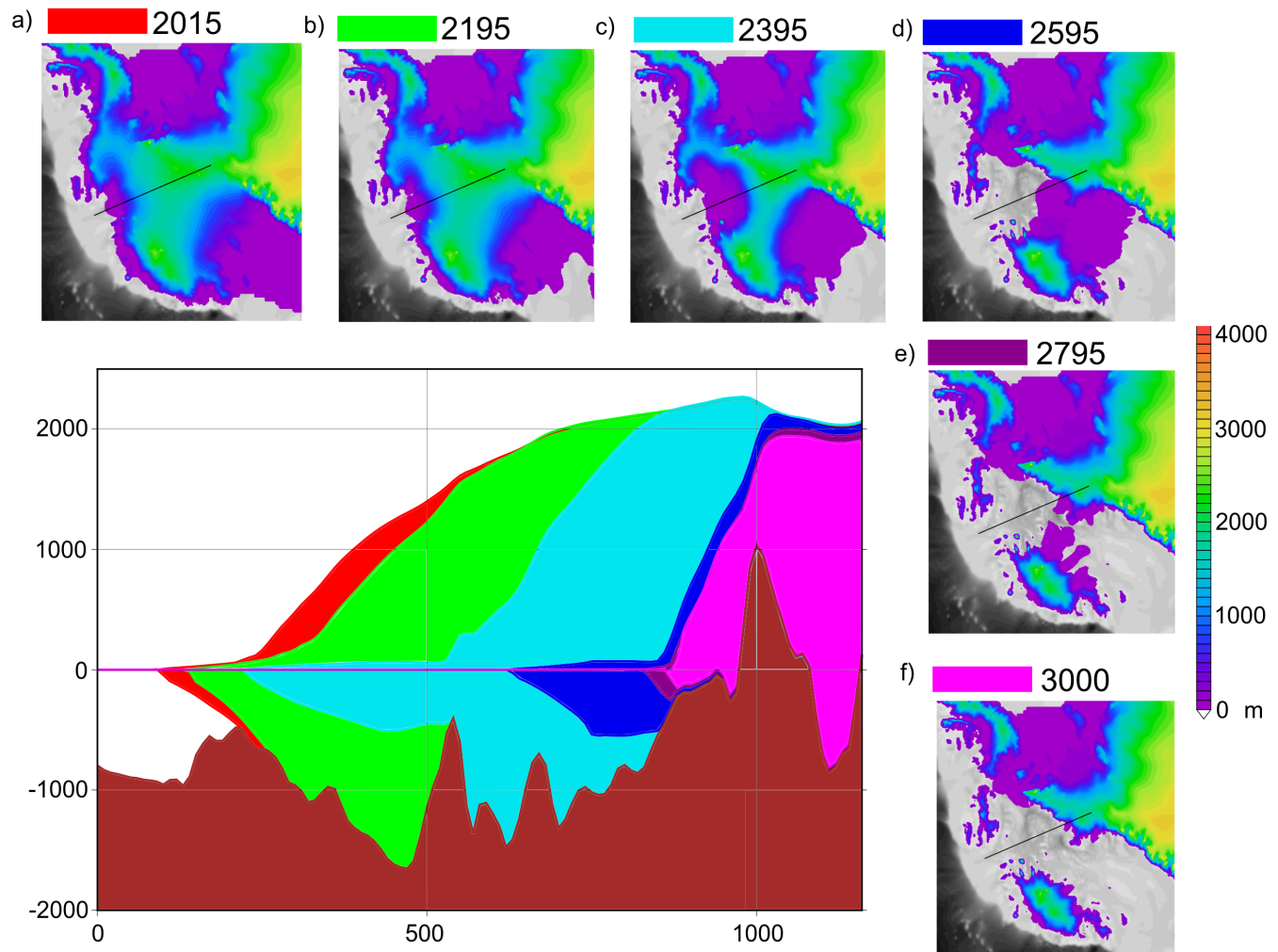


Fig. 6. Amundsen Embayment cross-section for simulation MIROC-ESM-CHEM RCP8.5 showing the ice extent for the years labeled in the side plots (a-f) which show the ice surface elevation for the year indicated.

215 case of the three, the CNRM-CM6 SSP5-8.5, which is also the only case that loses the Ronne-Filchner Ice
216 Shelf. The two CMIP5 RCP85 cases, the NORESM1-M and IPSL-CM5A-MR, are quite different from
217 each other with the NORESM1-M suffering much greater WAIS loss.

218 In Figure 8 the sea-level contributions by year 3000 are shown for each of 3 regions. Averaged across
219 all the high-emission cases, the WAIS contributes 3.2 m SLE compared with just 0.26 m from the EAIS
220 and 0.0044 m from the Antarctic Peninsula. This contrasts with the low-emission cases which have average
221 SLE contributions from the WAIS and EAIS of 0.086 and 0.12 m respectively, with the Antarctic Peninsula
222 contribution being very slightly negative at -0.0020 m SLE.

223 In addition to the standard ISMIP6 simulation set up, which includes a “medium” ice-shelf basal melt
224 calibration, two additional simulations under the NorESM1-M/RCP8.5 atmospheric forcing are run with
225 “high” and “low” ice-shelf basal melt calibrations. The results are shown by the green line (“medium”) and
226 green-shaded region (“high” is the top edge of the shading and “low” the bottom) in Figure 3. Decreasing
227 the ice-shelf basal melt causes a delay in the onset of the phase transitions when comparing “high” and
228 “low”, which produces a maximum sea-level contribution difference between “high” and “low”, during early
229 phase 4, of ~ 70 cm. The “medium” standard case behaves slightly differently, lining up closely with the
230 “high” case during early phase 4. Despite these differences all calibrations gradually converge during phase
231 4 such that the sea-level contributions end up only ~ 20 cm different by year 3000.

232 A more extreme test is NorESM1-M RCP8.5 with the “PIGL-medium” calibration. In this case phase
233 2 onset begins earlier than the other cases and lies well within the 21st century during the original ISMIP6
234 simulation period. As noted in Greve and others (2020), “It has a pronounced effect on the mass loss of
235 the ice sheet: By 2100, it is 216.7 mm SLE compared to the initial 1990 state”. In this case the transition
236 between phase 2 and 3 is unclear or absent and while there is some slowing to the increase in sea-level
237 contribution marking phase 4, sea-level contribution continues to increase at a relatively constant rate such
238 that by the year 3000 its total contribution is 5.4 m, the greatest of any of the cases. The reason for this
239 greater and continuing loss is in part because this case produces EAIS losses in the Amery and Wilkes
240 basins that are ongoing by the simulation end.

241 3.2 Extended ABUMIP experiments

242 For the extended ABUMIP simulations, ice thicknesses at the end of the simulations are shown in Figure 9.
243 The ice-shelf removal (abuk, abukiso) and extremely high ice-shelf melt (abum, abumiso) both show great

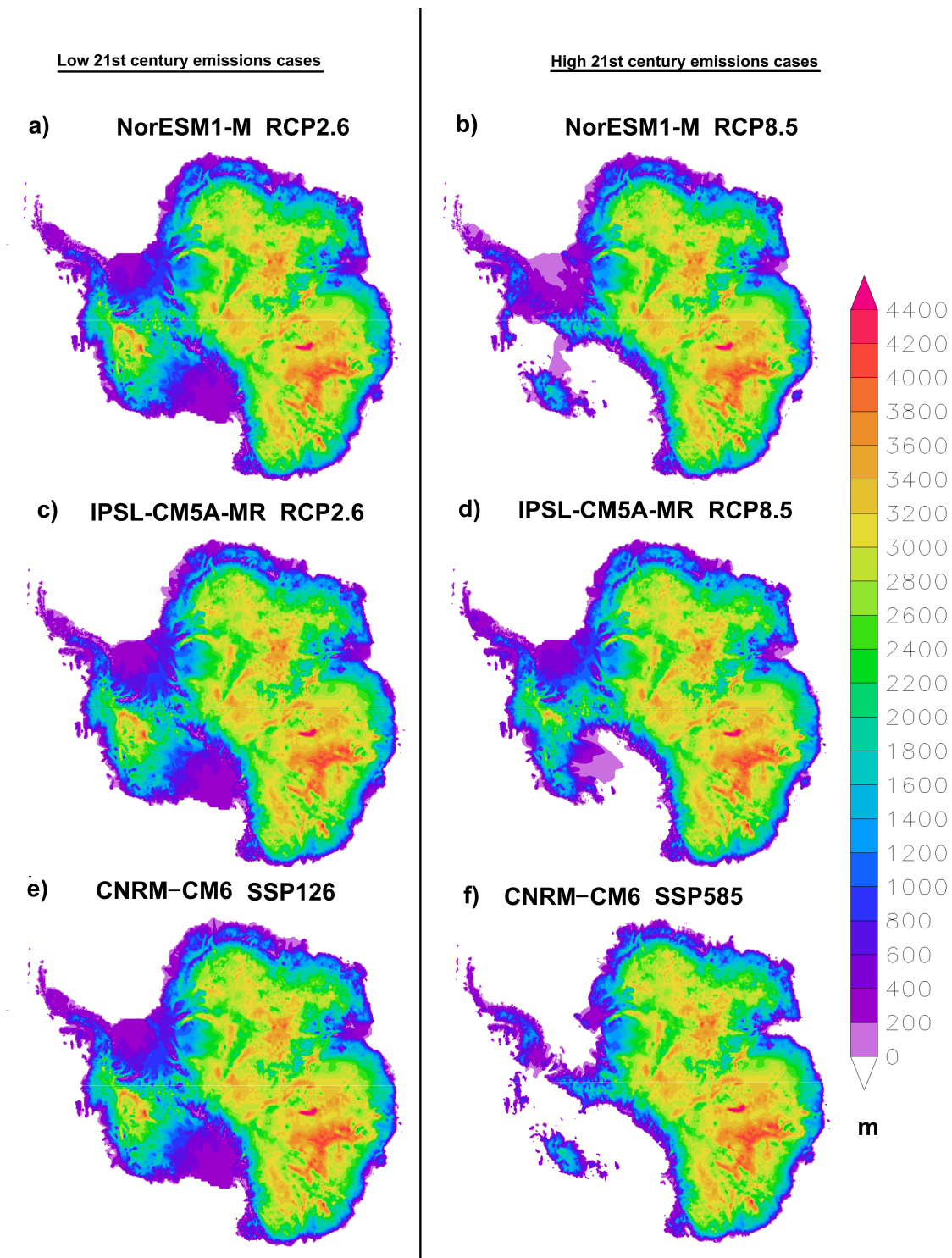


Fig. 7. Ice thickness at year 3000 for emissions reduction cases (left) and their counterpart high-emission cases (right).

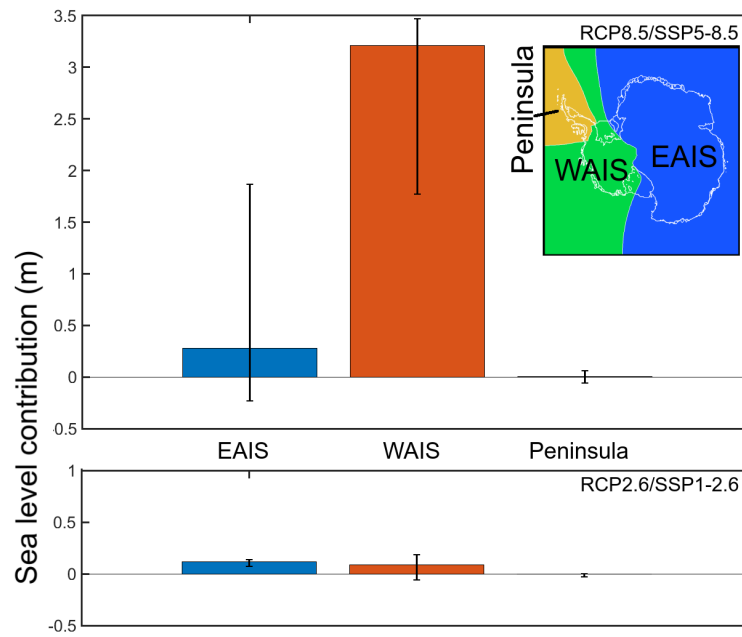


Fig. 8. Sea-level equivalent contribution from 3 regions (shown in top right) by year 3000 relative to ctrl_proj averaged across all the high (RCP8.5/SSP5-8.5, top) and low (RCP2.6/SSP1-2.6, bottom) emission cases. The whiskers show the full range of sea-level contributions across the simulations that make up the average.

244 changes to the ice sheet. In contrast to the extended ISMIP6 simulations, there are considerable losses
 245 in the EAIS in some of the regions where the ice is grounded below sea level. All extended ABUMIP
 246 simulations produce retreat inwards from the Amery Ice Shelf, however only in abum and abumiso is there
 247 a substantial retreat in the Wilkes Basin. These regions of greatest retreat are consistent with the original
 248 ABUMIP experiments in Sun and others (2020, Figs. 2 and 3) while being somewhat expanded given the
 249 longer simulation period.

250 Both the float kill, and extreme ice shelf melt cases were run with (abumiso, abukiso), and without,
 251 bedrock rebound (abum, abuk). Bedrock rebound occurs during, and after, ice-sheet mass loss, with the
 252 greatest amount reaching ~200 m of lift in central West Antarctica shown in Figure 10. The Aurora
 253 Basin, in particular, shows a large difference in ice-sheet loss with and without rebound (Fig. 9a,b), yet it
 254 experiences less rebound than other areas of major ice loss.

255 In fact the greatest differences in ice-sheet structure develop over the EAIS, and this seems to be due
 256 to the slower response of the ice sheet compared to the WAIS allowing a greater cumulative impact from
 257 rebound to develop. In Figure 10 the velocity difference due to rebound indicates large regions where
 258 bedrock rebound has slowed surface velocities in the Aurora Basin and also the Amery, Slessor, Recovery,

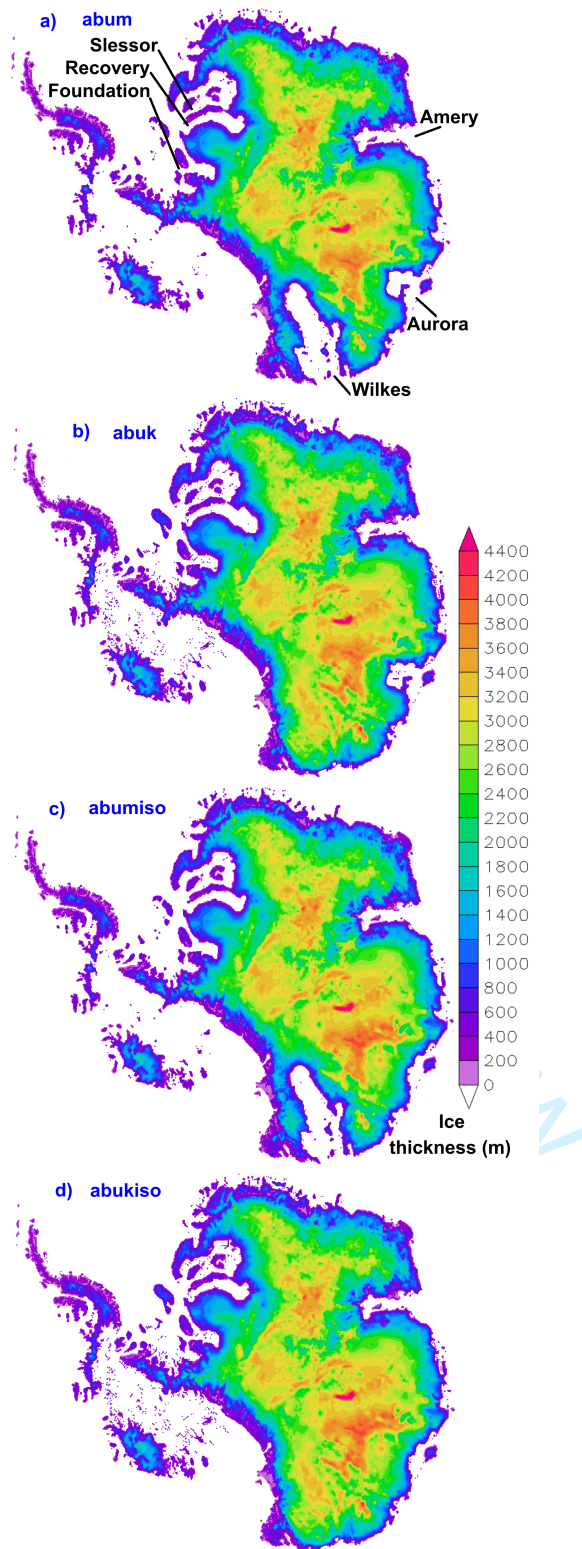


Fig. 9. ABUMIP ice thickness for year 3000 for a) abum, b) abuk, c) abumiso, and d) abukiso.

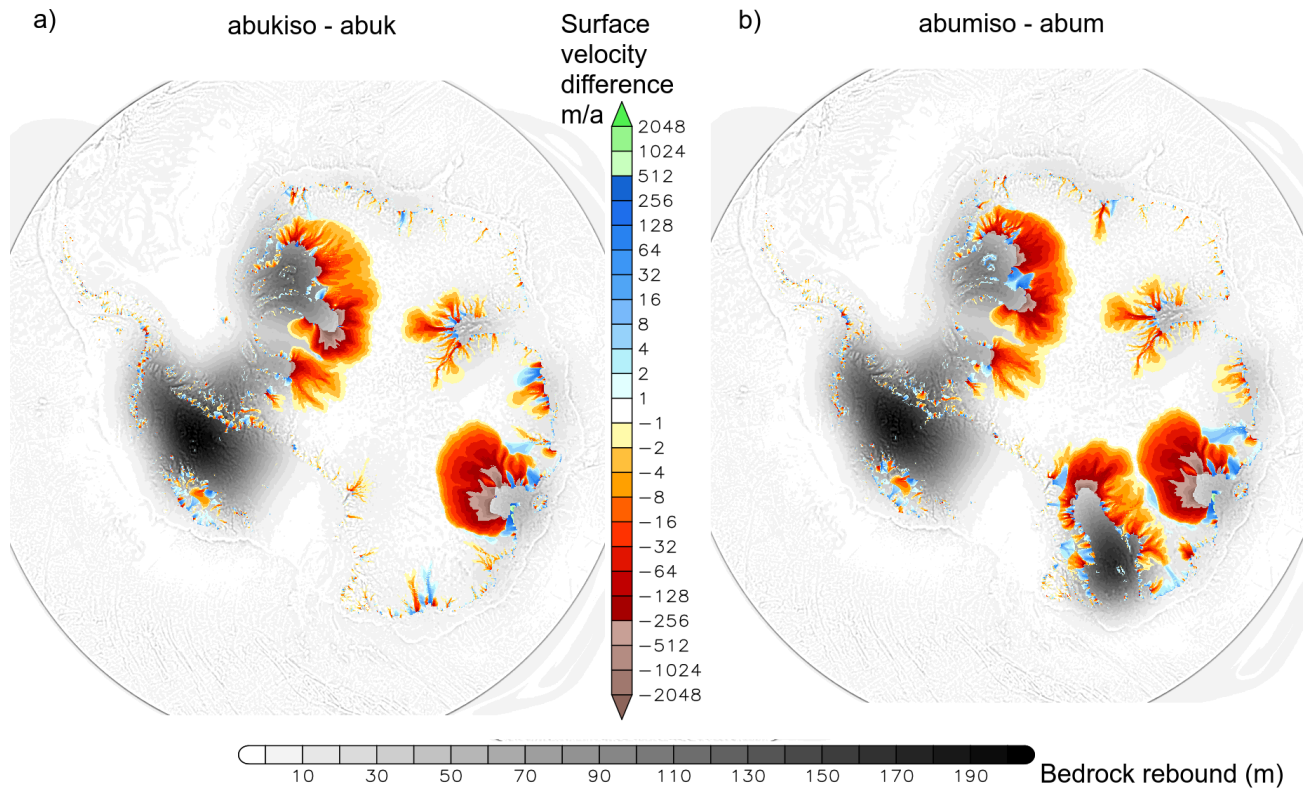


Fig. 10. Surface velocity differences between the ABUMIP bedrock rebound cases and the no rebound cases for the final simulation year (1000 years from 1990). Velocity differences are only plotted where ice exists in both the simulations. Underlain in gray shades is the bedrock rebound for a) abukiso and b) abumiso.

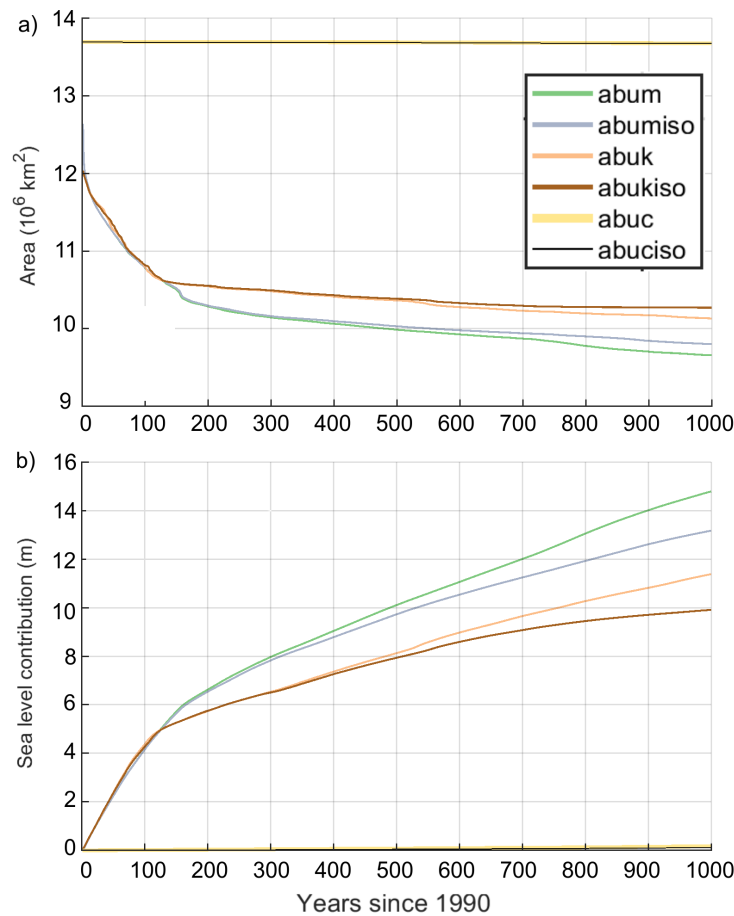


Fig. 11. ABUMIP a) total (grounded + floating) ice area and b) sea-level equivalent contribution.

259 and Foundation basins. Apparently, there is a critical stability occurring due to the topographic details in
 260 the region.

261 The cases without rebound gradually lose a greater area of ice over the course of the simulations and
 262 end up with $\sim 1.5 \times 10^5$ km² less ice sheet area (Fig. 11a). Overall the cases with rebound lose about 1.5
 263 metres less SLE (Fig. 11b).

264 4 DISCUSSION

265 The extended ISMIP6 experiments show the simulated long-term effect of applying a climate based on the
 266 last 10 years of the 21st century from the unabated warming and reduced emissions climate change scenarios.
 267 The simulations apply the assumption of no climate warming or cooling beyond year 2100. While using
 268 the same data from ISMIP6, the long-term picture is different from the 21st century ISMIP6 experiments
 269 showing that it is only in the long term that the consequence of different 21st century emission scenarios

270 becomes strikingly apparent. Under the unabated warming scenario, the AIS undergoes ice mass loss
271 primarily in the WAIS with the rate of loss divided into the 4 phases as detailed in the results. SICOPOLIS
272 is rather insensitive in the Amundsen Embayment due to the applied surface mass balance correction which
273 has additional accumulation to prevent the Thwaites/Pine Island glaciers from becoming unstable before
274 the end of the spin-up simulations. It is possible that this reduces the rate of ice-sheet collapse in the
275 Amundsen Embayment as compared to in the Ross Sea Embayment. Regardless, SICOPOLIS appears to
276 be simulating a marine-ice-sheet instability in these regions where the bed has a reverse slope and an initial
277 retreat increases discharge while reducing the balance flux, leading to grounding line thinning and further
278 retreat (e.g. Schoof, 2007). In the reduced emission scenarios the WAIS collapse does not occur indicating
279 that a climate threshold for large WAIS loss exists and that the 2091-2100 forcing in the reduced emission
280 cases is below this threshold.

281 In addition to the triggering of marine-ice-sheet instability, as ice warms its viscosity decreases which
282 can increase deformation rates and facilitate basal sliding leading to “creep instability”. The most im-
283 portant negative feedback opposing these positive feedbacks is due to increased precipitation in warming
284 temperatures which has been both observed (e.g. Frieler and others, 2015) and projected for the future,
285 over the Antarctic continent (Krinner and others, 2007; Uotila and others, 2007; Ligtenberg and others,
286 2013).

287 Beyond 2100, randomly chosen surface atmospheric forcings from 2091 to 2100 are used which means
288 that climate does not trend in time. RCP8.5 Projections beyond 2100 continue significant warming
289 (Bulthuis and others, 2019) that we do not consider here and is an avenue for future research. There
290 are no forcing modifications made due to the evolution of the surface topography which means that as
291 the WAIS ice sheet surface lowers, there is no increase in surface melt from an increase in temperature
292 expected due to the atmospheric lapse rate. As such the so-called “surface-melt-elevation feedback” (e.g.
293 Levermann and Winkelmann, 2016) is absent from these simulations. This effect should be most significant
294 where surface temperatures rise above freezing in confined areas around the edges of the ice sheet that
295 progress inward as the WAIS collapses in the high-emissions scenarios.

296 Potentially countering this absent positive feedback for ice loss, is the increase in freezing precipitation
297 that should penetrate inwards as the WAIS melts. This is due to the reduction in blocking topography, the
298 penetration of open ocean inwards increasing surface fluxes that feed precipitating clouds, the temperature
299 increase allowing the air to hold more water, and the thickening troposphere with a greater precipitable

300 water content. These limitations in the method applied here may be less problematic if the ice melt is
301 strongly dominated by ocean melt, as has been proposed before (e.g. Pritchard and others, 2012).

302 Mass budgets are included in the Appendix and indicate that mass loss is dominated by basal melting
303 of floating ice. This highlights the importance of correctly simulating sub-ice-shelf melt given that the Ross
304 Ice Shelf undergoes collapse during phase 2 of our simulations.

305 The extended ABUMIP results produce a greater loss in ice mass than the extended ISMIP6 simulations.
306 This acts as a longer demonstration of the importance of the buttressing of ice shelves on AIS mass loss
307 already seen in ABUMIP (Sun and others, 2020). The negative feedback from bedrock rebound is revealed
308 by these experiments, with a saving of about 1.5 m SLE by year 3000 attributable to it. This feedback has
309 been well documented in prior research (Gomez and others, 2010; Konrad and others, 2013; de Boer and
310 others, 2014; Gomez and others, 2015; Larour and others, 2019) and is proposed to work in a couple of
311 ways. As ice melts, the removal of ice mass causes the bedrock to rebound upwards creating a reduction
312 in slope from nearby still ice-covered regions towards the newly ice-free, or ice-reduced regions. A reduced
313 slope should tend to reduce ice sliding towards the ice-reduced regions. In addition, a grounding line with
314 a raised bedrock due to ice-mass loss will lower or eliminate sea water volume there, potentially reducing
315 the basal lubrication, which could act to reduce ice outflow.

316 Changes to surface velocities due to bedrock rebound are dependent on the bed topography shape and
317 the distribution of the rebound. Predominantly, this effect acts to reduce surface velocities as described
318 above. However there are regions where bedrock rebound increases the slope towards the ocean and can
319 therefore act to increase ice sliding. For example on the northern coasts of the WAIS where ice remains,
320 regions of increased velocity can be seen in Figure 10. Therefore bedrock rebound causes a complicated
321 redistribution of ice producing regions of increased and decreased ice flow but dominated by the larger
322 areas where velocity decreases. These areas develop over the long term in the embayments large enough to
323 develop the relationship with rebound described above. Studies have found that the upper mantle under
324 the WAIS might be softer than elsewhere in Antarctica (van der Wal and others, 2015; Hay and others,
325 2017) and so might experience greater bedrock rebound. Therefore there is potential for these impacts on
326 the ice budget to be greater and more regionally dependent.

327 5 CONCLUSION

328 Ice-sheet simulations of extended versions of ISMIP6 future climate experiments for the AIS until the year
329 3000 have been analysed. The simulations use climate projections from the beginning of 2015 until the
330 end of 2100, after which no further climate trend is applied, with forcing selected randomly from the final
331 decade of the 21st century. For the unabated 21st century warming simulations, a large difference in the
332 vulnerability of East and West Antarctica develops over hundreds of years, with West Antarctica suffering
333 a much more severe ice loss than East Antarctica. In these cases, the mass loss amounts to an average
334 across the simulations of ~ 3.5 m SLE. For the optimistic pathway, the mean mass loss is ~ 0.24 m SLE.
335 The results are radically different to the unclear response projected over the ISMIP6 period, demonstrating
336 that the consequences of the high-emissions scenario are much greater in the long term if a sustained, late-
337 21st-century climate is assumed.

338 Under the unabated 21st century warming scenario the ice sheet progresses through 4 phases, that are
339 defined by differing rates of ice loss. The stages are attributable to how the WAIS loses mass in the Ross
340 Sea Embayment followed later by additional loss from the Amundsen Sea Embayment and an eventual
341 levelling-out in the rate of ice sheet loss once the majority of the WAIS has melted.

342 The ABUMIP experiments provide a demonstration of a bedrock rebound negative feedback that re-
343 duces ice loss in a similar manner as found in previous research. However bedrock rebound can lead to
344 faster ice flow in certain smaller areas where it acts to increase the slope towards the ocean. Limitations to
345 our study, pointing to possible directions for future work, include the lack of accounting for local climatic
346 changes in regions where ice-sheet collapse occurs causing a sharp drop in surface elevations with proba-
347 ble positive feedback from regional large surface temperature increases, and negative feedback from large
348 frozen precipitation increases.

349 SUPPLEMENTARY MATERIAL

350 Animations made using VAPOR (vapor.ucar.edu) using the NorESM forcing are included as supplementary
351 material. Frame interval is 20 years. In these the RCP2.6 projection is labelled as “Optimistic” and RCP8.5
352 is labelled as “Pessimistic”.

353 Animation NorESMrebound.mp4

354 RCP8.5 ice thickness (m) and bedrock rebound (m, colour scale in key).

- 355 Animation NorESMthick.mp4
356 RCP2.6 vs RCP8.5 comparison of ice thickness (m).
- 357 Animation NorESMthickchange.mp4
358 RCP2.6 vs RCP8.5 comparison of ice thickness difference from 2015 (m).
- 359 Animation NorESMvhs.mp4
360 RCP2.6 vs RCP8.5 comparison of surface ice velocity (m a^{-1}).

361 ACKNOWLEDGEMENTS

362 We thank the Climate and Cryosphere (CliC) effort, which provided support for ISMIP6 through sponsoring
363 of workshops, hosting the ISMIP6 website and wiki, and promoting ISMIP6. We acknowledge the World
364 Climate Research Programme, which, through its Working Group on Coupled Modelling, coordinated and
365 promoted CMIP5 and CMIP6. We thank the climate modelling groups for producing their model output
366 and making it available; the Earth System Grid Federation (ESGF) for archiving the CMIP data and
367 providing access to it; the University at Buffalo for ISMIP6 data distribution and upload; and the multiple
368 funding agencies who support CMIP5, CMIP6, and ESGF. We thank the ISMIP6 steering committee, the
369 ISMIP6 model selection group and ISMIP6 dataset preparation group for their continuous engagement in
370 defining ISMIP6. This is ISMIP6 contribution No. xxx.

371 Christopher Chambers, Ralf Greve and Ayako Abe-Ouchi were supported by Japan Society for the
372 Promotion of Science (JSPS) KAKENHI Grant No. JP17H06323. Ralf Greve and Ayako Abe-Ouchi were
373 supported by JSPS KAKENHI Grant No. JP17H06104. Takashi Obase, Fuyuki Saito and Ayako Abe-Ouchi
374 were supported by JSPS Grant-in-Aid for Japan–France Integrated Action Program (SAKURA Program)
375 No. JPJSBP120213203.

376 REFERENCES

- 377 Alley RB, Anandkrishnan S, Christianson K, Horgan HJ, Muto A, Parizek BR, Pollard D and Walker RT (2015)
378 Oceanic forcing of ice-sheet retreat: West Antarctica and more. *Annual Review of Earth and Planetary Sciences*,
379 **43**(1), 207–231 (doi: 10.1146/annurev-earth-060614-105344)
- 380 Bamber JL, Riva REM, Vermeersen BLA and LeBrocq AM (2009) Reassessment of the potential sea-level rise from
381 a collapse of the West Antarctic Ice Sheet. *Science*, **324**(5929), 901–903 (doi: 10.1126/science.1169335)

- 382 Barthel A, Agosta C, Little CM, Hattermann T, Jourdain NC, Goelzer H, Nowicki S, Seroussi H, Straneo F and
383 Bracegirdle TJ (2020) CMIP5 model selection for ISMIP6 ice sheet model forcing: Greenland and Antarctica. *The*
384 *Cryosphere*, **14**(3), 855–879 (doi: 10.5194/tc-14-855-2020)
- 385 Bernales J, Rogozhina I, Greve R and Thomas M (2017) Comparison of hybrid schemes for the combination of
386 shallow approximations in numerical simulations of the Antarctic Ice Sheet. *The Cryosphere*, **11**(1), 247–265 (doi:
387 10.5194/tc-11-247-2017)
- 388 Bulthuis K, Arnst M, Sun S and Pattyn F (2019) Uncertainty quantification of the multi-centennial response of the
389 antarctic ice sheet to climate change. *The Cryosphere*, **13**(4), 1349–1380 (doi: 10.5194/tc-13-1349-2019)
- 390 Calov R, Beyer S, Greve R, Beckmann J, Willeit M, Kleiner T, Rückamp M, Humbert A and Ganopolski A (2018)
391 Simulation of the future sea level contribution of Greenland with a new glacial system model. *The Cryosphere*,
392 **12**(10), 3097–3121 (doi: 10.5194/tc-12-3097-2018)
- 393 de Boer B, Stocchi P and van de Wal RSW (2014) A fully coupled 3-D ice-sheet–sea-level model: algorithm and
394 applications. *Geoscientific Model Development*, **7**(5), 2141–2156 (doi: 10.5194/gmd-7-2141-2014)
- 395 Dutton A, Carlson AE, Long AJ, Milne GA, Clark PU, DeConto R, Horton BP, Rahmstorf S and Raymo ME
396 (2015) Sea-level rise due to polar ice-sheet mass loss during past warm periods. *Science*, **349**(6244), aaa4019 (doi:
397 10.1126/science.aaa4019)
- 398 Edwards TL, Nowicki S, Marzeion B, Hock R, Goelzer H, Seroussi H, Jourdain NC, Slater DA, Turner FE, Smith CJ,
399 McKenna CM, Simon E, Abe-Ouchi A, Gregory JM, Larour E, Lipscomb WH, Payne AJ, Shepherd A, Agosta C,
400 Alexander P, Albrecht T, Anderson B, Asay-Davis X, Aschwanden A, Barthel A, Bliss A, Calov R, Chambers C,
401 Champollion N, Choi Y, Cullather R, Cuzzzone J, Dumas C, Felikson D, Fettweis X, Fujita K, Galton-Fenzi BK,
402 Gladstone R, Golledge NR, Greve R, Hattermann T, Hoffman MJ, Humbert A, Huss M, Huybrechts P, Immerzeel
403 W, Kleiner T, Kraaijenbrink P, Le clec’h S, Lee V, Leguy GR, Little CM, Lowry DP, Malles JH, Martin DF,
404 Maussion F, Morlighem M, O’Neill JF, Nias I, Pattyn F, Pelle T, Price SF, Quiquet A, Radić V, Reese R, Rounce
405 DR, Rückamp M, Sakai A, Shafer C, Schlegel NJ, Shannon S, Smith RS, Straneo F, Sun S, Tarasov L, Trusel LD,
406 Van Breedam J, van de Wal R, van den Broeke M, Winkelmann R, Zekollari H, Zhao C, Zhang T and Zwinger
407 T (2021) Projected land ice contributions to twenty-first-century sea level rise. *Nature*, **593**(7857), 74–82 (doi:
408 10.1038/s41586-021-03302-y)
- 409 Eyring V, Bony S, Meehl GA, Senior CA, Stevens B, Stouffer RJ and Taylor KE (2016) Overview of the Coupled Model
410 Intercomparison Project Phase 6 (CMIP6) experimental design and organization. *Geoscientific Model Development*,
411 **9**(5), 1937–1958 (doi: 10.5194/gmd-9-1937-2016)

- 412 Fretwell P, Pritchard HD, Vaughan DG, Bamber JL, Barrand NE, Bell R, Bianchi C, Bingham RG, Blankenship DD,
413 Casassa G, Catania G, Callens D, Conway H, Cook AJ, Corr HFJ, Damaske D, Damm V, Ferraccioli F, Forsberg
414 R, Fujita S, Gim Y, Gogineni P, Griggs JA, Hindmarsh RCA, Holmlund P, Holt JW, Jacobel RW, Jenkins A,
415 Jokat W, Jordan T, King EC, Kohler J, Krabill W, Riger-Kusk M, Langley KA, Leitchenkov G, Leuschen C,
416 Luyendyk BP, Matsuoka K, Mouginot J, Nitsche FO, Nogi Y, Nost OA, Popov SV, Rignot E, Rippin DM, Rivera
417 A, Roberts J, Ross N, Siegert MJ, Smith AM, Steinhage D, Studinger M, Sun B, Tinto BK, Welch BC, Wilson
418 D, Young DA, Xiangbin C and Zirizzotti A (2013) Bedmap2: improved ice bed, surface and thickness datasets for
419 Antarctica. *The Cryosphere*, **7**(1), 375–393 (doi: 10.5194/tc-7-375-2013)
- 420 Frieler K, Clark PU, He F, Buizert C, Reese R, Ligtenberg SRM, van den Broeke MR, Winkelmann R and Levermann
421 A (2015) Consistent evidence of increasing Antarctic accumulation with warming. *Nature Climate Change*, **5**(4),
422 348–352 (doi: 10.1038/nclimate2574)
- 423 Garbe J, Albrecht T, Levermann A, Donges JF and Winkelmann R (2020) The hysteresis of the Antarctic Ice Sheet.
424 *Nature*, **585**(7826), 538–544 (doi: 10.1038/s41586-020-2727-5)
- 425 Gasson E, DeConto RM, Pollard D and Levy RH (2016) Dynamic Antarctic ice sheet during the early to mid-Miocene.
426 *Proceedings of the National Academy of Sciences*, **113**(13), 3459–3464 (doi: 10.1073/pnas.1516130113)
- 427 Golledge NR, Kowalewski DE, Naish TR, Levy RH, Fogwill CJ and Gasson EGW (2015) The multi-millennial
428 Antarctic commitment to future sea-level rise. *Nature*, **526**(7573), 421–425 (doi: 10.1038/nature15706)
- 429 Gomez N, Mitrovica JX, Huybers P and Clark PU (2010) Sea level as a stabilizing factor for marine-ice-sheet
430 grounding lines. *Nature Geoscience*, **3**(12), 850–853 (doi: 10.1038/ngeo1012)
- 431 Gomez N, Pollard D and Holland D (2015) Sea-level feedback lowers projections of future Antarctic Ice-Sheet mass
432 loss. *Nature Communications*, **6**(1), 8798 (doi: 10.1038/ncomms9798)
- 433 Greve R (1995) *Thermomechanisches Verhalten polythermer Eisschilde – Theorie, Analytik, Numerik*. Doctoral thesis,
434 Department of Mechanics, Darmstadt University of Technology, Germany (doi: 10.5281/zenodo.3815324)
- 435 Greve R (1997) Application of a polythermal three-dimensional ice sheet model to the Greenland ice sheet: Re-
436 sponse to steady-state and transient climate scenarios. *Journal of Climate*, **10**(5), 901–918 (doi: 10.1175/1520-
437 0442(1997)010<0901:AOAPTD>2.0.CO;2)
- 438 Greve R and SICOPOLIS Developer Team (2021) SICOPOLIS. GitLab, Alfred Wegener Institute for Polar and
439 Marine Research, Bremerhaven, Germany, URL <https://gitlab.awi.de/sicopolis/sicopolis>
- 440 Greve R, Calov R, Obase T, Saito F, Tsutaki S and Abe-Ouchi A (2020) ISMIP6 future projections for the Antarctic
441 ice sheet with the model SICOPOLIS. Technical report, Zenodo (doi: 10.5281/zenodo.3971232)

- 442 Hay CC, Lau HCP, Gomez N, Austermann J, Powell E, Mitrovica JX, Latychev K and Wiens DA (2017) Sea level
443 fingerprints in a region of complex earth structure: The case of wais. *Journal of Climate*, **30**(6), 1881 – 1892 (doi:
444 10.1175/JCLI-D-16-0388.1)
- 445 Joughin I and Alley RB (2011) Stability of the West Antarctic ice sheet in a warming world. *Nature Geoscience*,
446 **4**(8), 506–513 (doi: 10.1038/ngeo1194)
- 447 Joughin I, Smith BE and Medley B (2014) Marine ice sheet collapse potentially under way for the Thwaites Glacier
448 Basin, West Antarctica. *Science*, **344**(6185), 735–738 (doi: 10.1126/science.1249055)
- 449 Jourdain NC, Asay-Davis X, Hattermann T, Straneo F, Seroussi H, Little CM and Nowicki S (2020) A protocol for
450 calculating basal melt rates in the ISMIP6 Antarctic ice sheet projections. *The Cryosphere*, **14**(9), 3111–3134 (doi:
451 10.5194/tc-14-3111-2020)
- 452 Konrad H, Thoma M, Sasgen I, Klemann V, Grosfeld K, Barbi D and Martinec Z (2013) The deformational response
453 of a viscoelastic solid earth model coupled to a thermomechanical ice sheet model. *Surveys in Geophysics* (doi:
454 10.1007/s10712-013-9257-8)
- 455 Krinner G, Magand O, Simmonds I, Genthon C and Dufresne JL (2007) Simulated Antarctic precipitation and
456 surface mass balance at the end of the twentieth and twenty-first centuries. *Climate Dynamics*, **28**(2-3), 215–230
457 (doi: 10.1007/s00382-006-0177-x)
- 458 Larour E, Seroussi H, Adhikari S, Ivins E, Caron L, Morlighem M and Schlegel N (2019) Slowdown in antarctic mass
459 loss from solid earth and sea-level feedbacks. *science*, **364**(6444) (doi: 10.1126/science.aav7908)
- 460 Levermann A and Winkelmann R (2016) A simple equation for the melt elevation feedback of ice sheets. *The*
461 *Cryosphere*, **10**(4), 1799–1807 (doi: 10.5194/tc-10-1799-2016)
- 462 Levermann A, Clark PU, Marzeion B, Milne GA, Pollard D, Radic V and Robinson A (2013) The multimillennial
463 sea-level commitment of global warming. *Proceedings of the National Academy of Sciences*, **110**(34), 13745–13750
464 (doi: 10.1073/pnas.1219414110)
- 465 Ligtenberg SRM, van de Berg WJ, van den Broeke MR, Rae JGL and van Meijgaard E (2013) Future surface mass
466 balance of the Antarctic ice sheet and its influence on sea level change, simulated by a regional atmospheric climate
467 model. *Climate Dynamics*, **41**(3-4), 867–884 (doi: 10.1007/s00382-013-1749-1)
- 468 Lipscomb WH, Leguy GR, Jourdain NC, Asay-Davis X, Seroussi H and Nowicki S (2021) ISMIP6-based projections of
469 ocean-forced Antarctic Ice Sheet evolution using the Community Ice Sheet Model. *The Cryosphere*, **15**(2), 633–661
470 (doi: 10.5194/tc-15-633-2021)

- 471 Mercer JH (1968) Antarctic ice and Sangamon sea level. In *Bern General Assembly, Commission of Snow and Ice*,
472 1967, IAHS Publication No. 79, 217–225, International Association of Hydrological Sciences
- 473 Nowicki S, Goelzer H, Seroussi H, Payne AJ, Lipscomb WH, Abe-Ouchi A, Agosta C, Alexander P, Asay-Davis
474 XS, Barthel A, Bracegirdle TJ, Cullather R, Felikson D, Fettweis X, Gregory JM, Hattermann T, Jourdain NC,
475 Kuipers Munneke P, Larour E, Little CM, Morlighem M, Nias I, Shepherd A, Simon E, Slater D, Smith RS, Straneo
476 F, Trusel LD, van den Broeke MR and van de Wal R (2020) Experimental protocol for sea level projections from
477 ISMIP6 stand-alone ice sheet models. *The Cryosphere*, **14**(7), 2331–2368 (doi: 10.5194/tc-14-2331-2020)
- 478 Nowicki SMJ, Payne A, Larour E, Seroussi H, Goelzer H, Lipscomb W, Gregory J, Abe-Ouchi A and Shepherd A
479 (2016) Ice Sheet Model Intercomparison Project (ISMIP6) contribution to CMIP6. *Geoscientific Model Develop-*
480 *ment*, **9**(12), 4521–4545 (doi: 10.5194/gmd-9-4521-2016)
- 481 Payne AJ, Nowicki S, Abe-Ouchi A, Agosta C, Alexander P, Albrecht T, Asay-Davis X, Aschwanden A, Barthel
482 A, Bracegirdle TJ, Calov R, Chambers C, Choi Y, Cullather R, Cuzzone J, Dumas C, Edwards TL, Felikson
483 D, Fettweis X, Galton-Fenzi BK, Goelzer H, Gladstone R, Golledge NR, Gregory JM, Greve R, Hattermann T,
484 Hoffman MJ, Humbert A, Huybrechts P, Jourdain NC, Kleiner T, Munneke PK, Larour E, Le clec'h S, Lee V,
485 Leguy G, Lipscomb WH, Little CM, Lowry DP, Morlighem M, Nias I, Pattyn F, Pelle T, Price SF, Quiquet A,
486 Reese R, Rückamp M, Schlegel NJ, Seroussi H, Shepherd A, Simon E, Slater D, Smith RS, Straneo F, Sun S,
487 Tarasov L, Trusel LD, Van Breedam J, van de Wal R, van den Broeke M, Winkelmann R, Zhao C, Zhang T and
488 Zwinger T (2021) Future sea level change under CMIP5 and CMIP6 scenarios from the Greenland and Antarctic
489 ice sheets. *Geophysical Research Letters* (doi: 10.1029/2020GL091741), in press
- 490 Pollard D and DeConto RM (2009) Modelling West Antarctic ice sheet growth and collapse through the past five
491 million years. *Nature*, **458**(7236), 329–332 (doi: 10.1038/nature07809)
- 492 Pritchard HD, Ligtenberg SRM, Fricker HA, Vaughan DG, van den Broeke MR and Padman L (2012) Antarctic
493 ice-sheet loss driven by basal melting of ice shelves. *Nature*, **484**(7395), 502–505 (doi: 10.1038/nature10968)
- 494 Rignot E and Mouginot J (2016) Antarctica and Greenland drainage basin and ice sheet definitions. IMBIE 2016
- 495 Rignot E, Mouginot J, Morlighem M, Seroussi H and Scheuchl B (2014) Widespread, rapid grounding line retreat
496 of Pine Island, Thwaites, Smith, and Kohler glaciers, West Antarctica, from 1992 to 2011. *Geophysical Research*
497 *Letters*, **41**(10), 3502–3509 (doi: 10.1002/2014GL060140)
- 498 Sato T and Greve R (2012) Sensitivity experiments for the Antarctic ice sheet with varied sub-ice-shelf melting rates.
499 *Annals of Glaciology*, **53**(60), 221–228 (doi: 10.3189/2012AoG60A042)
- 500 Schaeffer M, Hare W, Rahmstorf S and Vermeer M (2012) Long-term sea-level rise implied by 1.5 °C and 2 °C
501 warming levels. *Nature Climate Change*, **2**(12), 867–870 (doi: 10.1038/nclimate1584)

- 502 Schoof C (2007) Ice sheet grounding line dynamics: Steady states, stability, and hysteresis. *Journal of Geophysical*
503 *Research: Earth Surface*, **112**(F3), F03S28 (doi: 10.1029/2006JF000664)
- 504 Seroussi H, Nowicki S, Payne AJ, Goelzer H, Lipscomb WH, Abe-Ouchi A, Agosta C, Albrecht T, Asay-Davis X,
505 Barthel A, Calov R, Cullather R, Dumas C, Galton-Fenzi BK, Gladstone R, Golledge N, Gregory JM, Greve R,
506 Hatterman T, Hoffman MJ, Humbert A, Huybrechts P, Jourdain NC, Kleiner T, Larour E, Leguy GR, Lowry DP,
507 Little CM, Morlighem M, Pattyn F, Pelle T, Price SF, Quiquet A, Reese R, Schlegel NJ, Shepherd A, Simon E,
508 Smith RS, Straneo F, Sun S, Trusel LD, Van Breedam J, van de Wal RSW, Winkelmann R, Zhao C, Zhang T and
509 Zwinger T (2020) ISMIP6 Antarctica: a multi-model ensemble of the Antarctic ice sheet evolution over the 21st
510 century. *The Cryosphere*, **14**(9), 3033–3070 (doi: 10.5194/tc-14-3033-2020)
- 511 Sun S, Pattyn F, Simon EG, Albrecht T, Cornford S, Calov R, Dumas C, Gillet-Chaulet F, Goelzer H, Golledge NR,
512 Greve R, Hoffman MJ, Humbert A, Kazmierczak E, Kleiner T, Leguy GR, Lipscomb WH, Martin D, Morlighem
513 M, Nowicki S, Pollard D, Price S, Quiquet A, Seroussi H, Schlemm T, Sutter J, van de Wal RSW, Winkelmann R
514 and Zhang T (2020) Antarctic ice sheet response to sudden and sustained ice-shelf collapse (ABUMIP). *Journal*
515 *of Glaciology*, **66**(260), 891–904 (doi: 10.1017/jog.2020.67)
- 516 The IMBIE team (2018) Mass balance of the Antarctic Ice Sheet from 1992 to 2017. *Nature*, **558**(7709), 219–222
517 (doi: 10.1038/s41586-018-0179-y)
- 518 Trusel LD, Frey KE, Das SB, Karnauskas KB, Kuipers Munneke P, van Meijgaard E and van den Broeke MR
519 (2015) Divergent trajectories of Antarctic surface melt under two twenty-first-century climate scenarios. *Nature*
520 *Geoscience*, **8**(12), 927–932 (doi: 10.1038/ngeo2563)
- 521 Turney CSM, Fogwill CJ, Golledge NR, McKay NP, van Sebille E, Jones RT, Etheridge D, Rubino M, Thornton DP,
522 Davies SM, Ramsey CB, Thomas ZA, Bird MI, Munksgaard NC, Kohno M, Woodward J, Winter K, Weyrich LS,
523 Rootes CM, Millman H, Albert PG, Rivera A, van Ommen T, Curran M, Moy A, Rahmstorf S, Kawamura K,
524 Hillenbrand CD, Weber ME, Manning CJ, Young J and Cooper A (2020) Early Last Interglacial ocean warming
525 drove substantial ice mass loss from Antarctica. *Proceedings of the National Academy of Sciences*, **117**(8), 3996–
526 4006 (doi: 10.1073/pnas.1902469117)
- 527 Uotila P, Lynch AH, Cassano JJ and Cullather RI (2007) Changes in Antarctic net precipitation in the 21st century
528 based on Intergovernmental Panel on Climate Change (IPCC) model scenarios. *Journal of Geophysical Research:*
529 *Atmospheres*, **112**(D10), D10107 (doi: 10.1029/2006JD007482)
- 530 van der Wal W, Whitehouse PL and Schrama EJ (2015) Effect of GIA models with 3D composite mantle viscosity
531 on GRACE mass balance estimates for Antarctica. *Earth and Planetary Science Letters*, **414**, 134–143 (doi:
532 10.1016/j.epsl.2015.01.001)

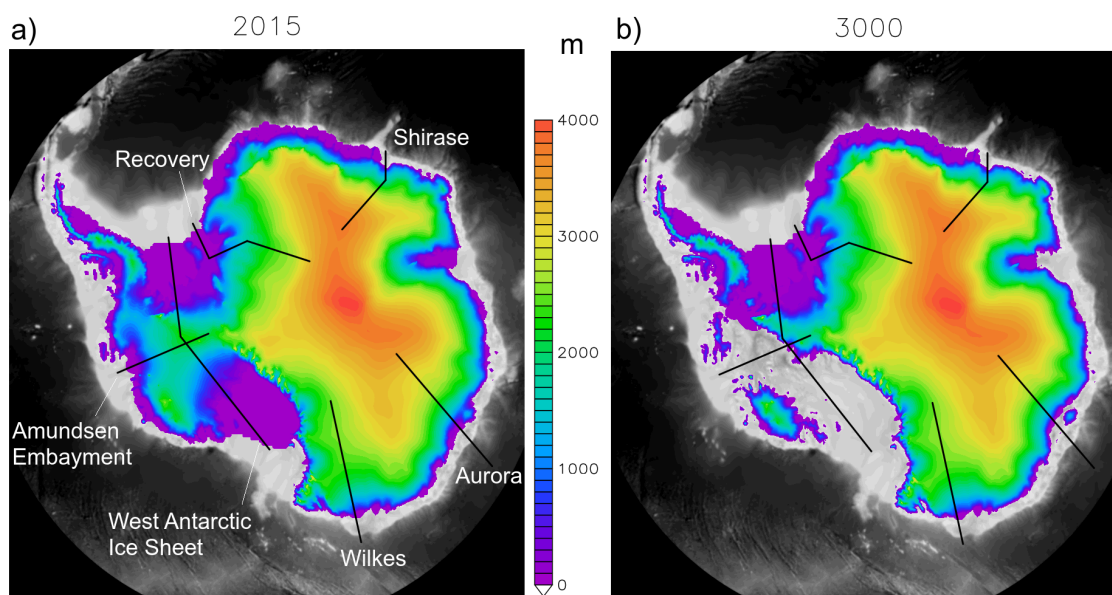


Fig. 12. Cross-section locations on surface topography for the MIROC-ESM-CHEM RCP8.5 experiment for a) 2015, and b) 3000. Included are cross-section locations for the WAIS used in Figure 4 and the Amundsen Embayment in Figure 6.

533 A APPENDIX

534 This appendix presents additional cross-sections and mass budgets for the MIROC-ESM-CHEM RCP8.5
 535 case. Considered first are four EAIS cross-sections, guided by the ice flow line, for the Recovery, Shirase,
 536 Aurora, and Wilkes basins. The locations of the cross-sections, as well as those shown earlier in Figures 4
 537 and 6, are in Figure 12. The cross-sections shown in Figure 13 all show far less change than those for the
 538 WAIS. In the extreme, the Shirase section shows so little ice change at the coast that all profiles from 2015
 539 to 3000 appear to overlap to form one line. The only change in this profile is from the slow thickening of
 540 the interior ice. The Recovery and Wilkes cross-sections show some minor ice shelf basal melt, however
 541 there again is essentially no coastal retreat. Of the four, the Aurora basin has the greatest response
 542 with ~ 150 km retreat in the ice at the coast. The loss in coastal ice, combined with the thickening of
 543 interior ice, steepens the ice sheet slopes slightly, with the greatest steepening in the Aurora basin. Further
 544 investigation is recommended to determine why so little simulated change is seen in East Antarctica.

545 Secondly, mass budgets are shown in Figure 14. The mass loss is driven almost entirely by basal mass
 546 loss from floating ice. Comparing the regionally divided figures indicates that the rapid ice loss during
 547 phase 3 is driven primarily by basal mass loss from floating ice in the WAIS. The sharp dip in the rate of

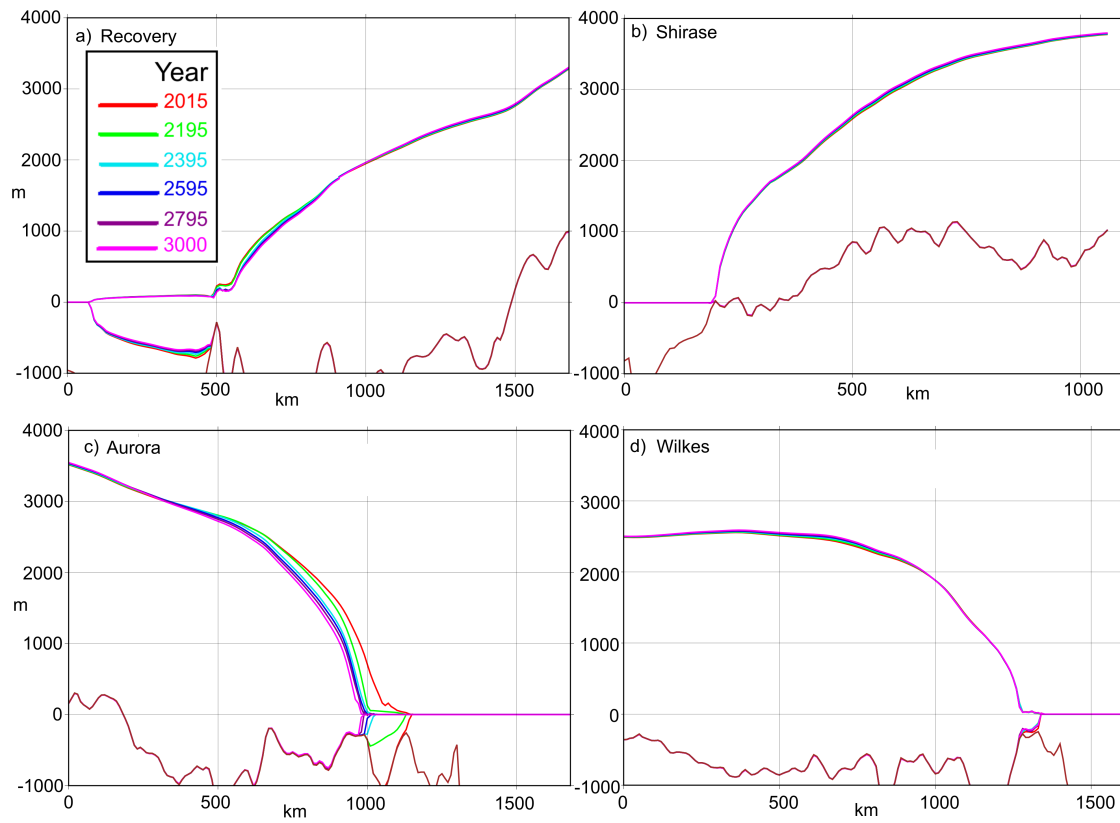


Fig. 13. EAIS ice profile cross-sections for a) Recovery, b) Shirase, c) Aurora, and d) Wilkes for the years indicated.

548 volume change around 2100 is associated with the transition from a warming climate to a constant climate.
549 The total surface mass balance declines between 2100 and 3000 over the WAIS. This may be due to the
550 reduction in surface ice area or the redistribution of ice away from areas of positive mass balance in the
551 end of 21st century forcing data used.

For Peer Review

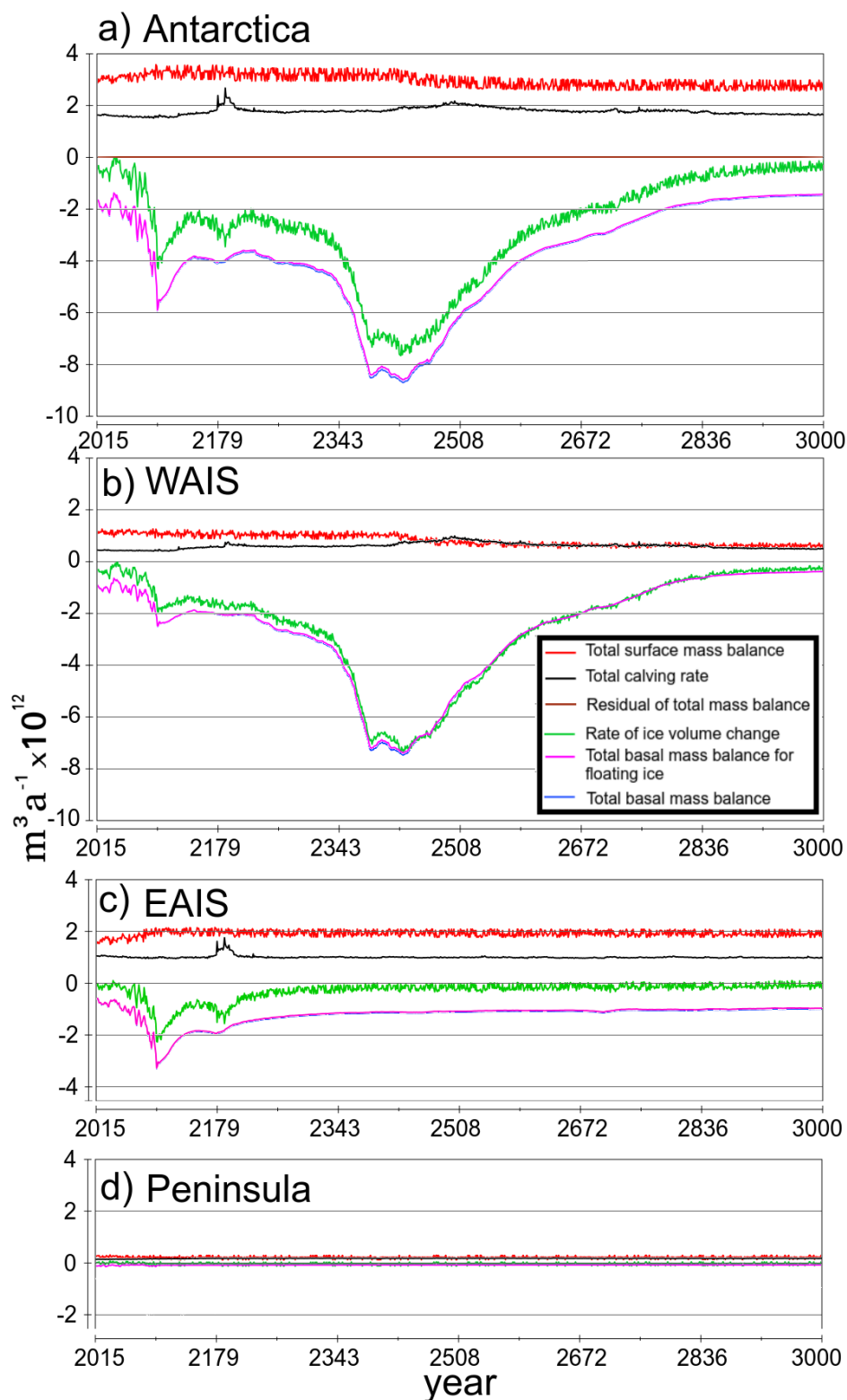


Fig. 14. Mass budget components for the MIROC-ESM-CHEM RCP8.5 case for a) all Antarctica, b) WAIS, c) EAIS, and d) the Antarctic Peninsula.